minerals

MDPI

Article

Research on Behavior of Iron in the Zinc Sulfide Pressure Leaching Process

Shu-Chen Qin [1], Kai-Xi Jiang [1,2,*], Hai-Bei Wang [1], Bang-Sheng Zhang [1], Yu-Fang Wang [1] and Xue-Dong Zhang [1]

[1] BGRIMM Technology Group, Beijing 100160, China; qshuchen@163.com (S.-C.Q.); whaibei_01@163.com (H.-B.W.); zbsvictory@163.com (B.-S.Z.); Wang_yf@bgrimm.com (Y.-F.W.); zhangxuedong92@yeah.net (X.-D.Z.)

[2] The College of Zijin Mining, Fuzhou University, Fuzhou 350108, China

* Correspondence: Jiangkx@bgrimm.com

Received: 13 December 2019; Accepted: 24 February 2020; Published: 29 February 2020

Abstract: Dissolved iron exerts significant effects on mineral leaching, impurity removal, and solution purification in the zinc hydrometallurgy process. To date, iron oxidation and migration behaviors are yet to be fully understood and further research on effective regulation mechanisms of iron is required. In this paper, zinc sulfide concentrate was used as the research object. The behaviors of both Zn and Fe during pressure leaching were investigated for varying temperature, acid addition, and leaching time. At temperature of 100~160 °C, H_2SO_4/Zn ratio of 0.9:1–1.25:1, and leaching time of 0.5–2.5 h, the zinc extraction increased with temperature, acidity and leaching time. The iron extraction, however, varied differently with increasing temperature, acidity and leaching time: (A) it increased with temperature to 150 °C and then decreased at higher temperature, and (B) displayed an initial increase followed by a decrease with respect to the leaching time. Based on the characteristics of the residue phase, chemical phase analysis was used to analyze the residue in detail. The extent of dissolution of iron-containing minerals and the extent of precipitation of ferric ions during the leaching process were quantitatively calculated.

Keywords: zinc sulfide concentrate; pressure leaching; iron extraction; iron hydrolysis

1. Introduction

Zinc is an important non-ferrous metal, second to copper and aluminum in the consumption of non-ferrous metals, mainly applied in steel, metallurgy, machinery, electrical, chemical, light industry, and military fields [1,2]. Currently, more than 85% of zinc is produced through the Roasting-Leaching-Electrowinning (RLE) process, which is the most important method of zinc extraction from sulfide ores and concentrates [3–6]. During this process, both the sulfide ores and concentrates are roasted at 700 to 900 °C, generating SO_2, which is known to be an environmental pollutant [7]. Pressure leaching is a promising process for reducing environmental pollution essentially by removing the roasting step from the RLE process thus producing elemental sulfur or sulfate instead of SO_2 [8,9].

In recent years, the application of pressure leaching technology by both domestic and foreign enterprises has enabled certain economic benefits to be achieved. For example, Yunnan Metallurgical Group (Kunming, China), Western Mining Co. (Xining, China) and other smelting companies have successively adopted pressure leaching technology to treat zinc ores. Zijin group (Shanghang, China) successfully put into operation the pressurized pre-oxidation treatment of gold ores 3 years ago, which has resulted in a 30% increase in the overall recovery and an estimated economic benefit of about 10 billion yuan. Throughout the pressure acid leaching process, iron existing in various minerals such

as sphalerite, chalcopyrite, and pyrrhotite is dissolved in the form of $FeSO_4$. As the oxidative leaching proceeds, the dissolved $FeSO_4$ is then oxidized to $Fe_2(SO_4)_3$. Since the processing temperatures of the pressure leaching process are generally high, the ferric iron is hydrolyzed to form various iron-containing phases. At lower temperatures, goethite is formed in solutions with low ferric ions (Fe^{3+}) concentrations, while hydronium jarosite is formed in solutions with high Fe^{3+} concentrations. Raising the temperature to 150 °C leads to the formation of hematite in solutions with low Fe^{3+} concentrations. The hydronium jarosite formed in solutions with high Fe^{3+} concentrations is highly unstable and usually breaks down to form $Fe_2O_3{\cdot}2SO_3{\cdot}H_2O$, i.e., basic ferric sulfate [10–14]. Other jarosite compounds can be formed when Na^+, K^+ and Pb^{2+} are present in solution [15–18]. It has been reported by E.G. Parker al. [19] that under conditions of 150 °C and low acidity, ferric ion precipitates as an alkaline bisulfate salt, and the type of precipitate phase formed highly varies according to the conditions. Industrially, the process conditions are regulated to reduce the iron content of the leach solution, and preferably precipitate iron in the form of goethite, hematite or jarosite.

A previous study on the leaching behavior of sphalerite by Xu Zhifeng et al. [20] indicated that the dissolution of iron-containing minerals and the hydrolysis-precipitation of dissolved iron occurs simultaneously by analyzing the surface properties of the sphalerite using the XPS method. At the initial stage of leaching, iron dissolution is dominant throughout the rest of the process. The iron precipitates in the residue are mostly in the form of amorphous iron oxide, which can be adjusted to meet the industrial requirements. Although many studies have investigated the leaching process of iron-containing minerals, most of these are limited to qualitatively predicting the iron phase changes in the residue sample. The quantitative explanation of iron-containing mineral behavior is still not well understood.

In this paper, the effects of temperature, acidity and duration on the pressure leaching process were evaluated with zinc sulfide concentrate. The behavior of zinc and iron throughout the pressure leaching process was investigated. The leach residue was analyzed using a chemical phase analysis method. Moreover, the extent of dissolution of iron-containing minerals and the extent of precipitation of ferric ions during the leaching process were quantitatively studied. The behavior of iron in the system was revealed and the reasons are briefly explained. This study enables the effective control and utilization of iron with certain technical basis.

2. Materials and Methods

2.1. Materials and Reagents

The zinc concentrate used in this study was supplied by a Sichuan Smelter. The main element compositions are shown in Table 1. The H_2SO_4, $FeSO_4$, and $CuSO_4$ used in the study were all analytically pure, and the oxygen and lignin were of industrial grade. The mineral sample was wet-milled for 15 min by conical mill (1 kg ore sample and 1 L water), until the particles reach the size of approximately −325 mesh accounting for 93%. The XRD pattern and SEM images of the morphologies of the zinc sulfide concentrate are shown in Figures 1 and 2. The main phases contained in the ore sample include sphalerite ($Zn_xFe_{1-x}S$), quartz (SiO_2), galena (PbS), pyrite (FeS_2) and chalcopyrite ($CuFeS_2$).

Table 1. Chemical composition of the ZnS concentrate.

Element	Zn	Fe	S	Cu	Pb	SiO_2	CaO	K_2O	Na_2O
Content/%	55.5	2.4	29.3	0.64	1.6	5.4	0.71	0.10	<0.10

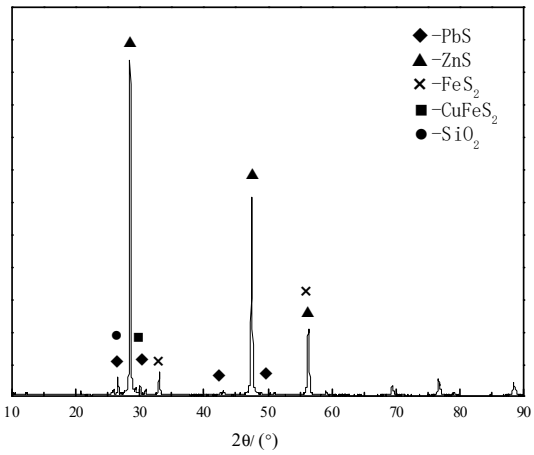

Figure 1. XRD pattern of the ZnS concentrate with identified mineral phases.

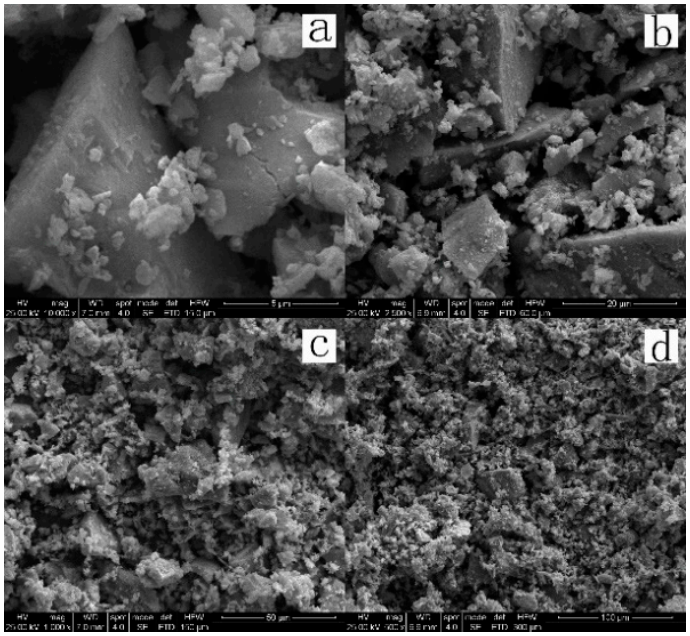

Figure 2. Morphologies of the ZnS concentrate. Scale: (**a**) 5 μm; (**b**) 20 μm; (**c**) 50 μm; (**d**) 100 μm.

2.2. Leaching Process

The pressure leaching experiment was carried out in a 2 L titanium lined autoclave (Shandong Weihai Chemical Machinery Co., Ltd., Weihai, China). A specific amount of ore and H_2SO_4 solution containing lignin were added into the autoclave. After stirring, the vessel integrity was checked by sealing the autoclave and then filling it with oxygen. A precise volume of oxygen was added into the autoclave in order to expel the gaseous impurity and maintain an oxygen-rich environment, thus protecting the titanium-lined autoclave from the corrosion produced by hydrogen sulfide gas. Next, the cooling water was connected and the power switched on. The rotation speed and temperature were set to their preset value. After the temperature reached the preset value, it was held for a certain duration. At the end of the experiment, the autoclave was cooled down to about 70 °C using pure water. The head space was discharged, and the slurry taken out of the autoclave. The slurry was vacuum filtered to separate solids from the leach liquor. The leach residue was washed with deionized water and placed in a drying oven at a constant temperature. The Zn and Fe contained in

the leach residue were analyzed and the metal leaching percentage extraction was obtained by using the following formula:

$$\eta = \frac{w_0 - w}{w_0} \times 100\%, \quad (1)$$

where, η is the leaching percentage, in %, ω_0 is the mass of the metal element in the raw ore in grams (g), and ω is the mass of the metal element in the residue in grams (g);

Lignin was added to the leaching process as this serves the functions of dispersing sulfur, eliminating sulfur agglomeration and minimizing the effect of sulfur covering the mineral. The addition of lignin in our experiment can therefore alleviate the effects of sulphur coating minerals and improve the extraction.

2.3. Calculation of Iron Deportment

The iron-containing minerals in zinc sulfide concentrates usually consist of sphalerite, chalcopyrite and pyrite, all of which are dissolved during the leaching process to form ferrous ions in the solution. The ferrous ions in the solution are oxidized and subsequently hydrolyzed to form hematite, as shown in the following reaction:

$$2FeSO_4 + 1/2O_2 + 2H_2O = Fe_2O_3 + 2H_2SO_4$$

If monovalent cations are present in the solution, the iron hydrolyzes to form jarosite-type compounds in the residue, as illustrated by the following reaction:

$$3Fe_2(SO_4)_3 + K_2SO_4 + 12H_2O = K_2Fe_6(SO_4)_4(OH)_{12} + 6H_2SO_4$$

It can be seen that the variation of iron arises from the combination of the leaching of iron-containing minerals and iron hydrolysis precipitation. The relationship between leaching and precipitation of iron can be written as follows:

$$Fe_{\text{ leached}} = Fe_{\text{ decomposed}} - Fe_{\text{ precipitated}}$$

$$Fe_{\text{ ore}} = Fe_{\text{ decomposed}} + Fe_{\text{ residual sulfide}}$$

The behavior of iron can be quantitatively determined using Equation (1), in which the amount of decomposed iron-containing minerals and the amount of precipitated iron from hydrolysis during the leaching process can be determined once the value for iron in the residual sulfide has been obtained.

2.4. Analysis and Detection

The phase composition of the ore and the leach residue samples were investigated by X-ray diffractometer (XRD, D/max-Ultima IV, Rigaku, Japan). The morphology of the samples was observed by scanning electron microscopy (SEM, Hitachi S-3500, Hitachi, Japan). The chemical states of Zn, Fe, and S in the residue were analyzed by X-ray energy dispersive spectroscopy (EDS, LINK-ISIS300, Oxford, UK). Residual acid concentration was determined by sodium hydroxide (NaOH) neutralization titration.

Based upon the leach residue phase composition characteristics, the traditional sulfur chemical state analysis method was improved. The sulfur and iron chemical phase analysis methods were integrated to determine the iron contents by analyzing the sulfide and sulfate species. The chemical states of sulfur and iron can be simultaneously identified. Meanwhile, the content of both iron and sulfur in the leach residue could also be simultaneously determined. The specific analysis process is to dissolve the soluble sulfate with NaCl solution and then dissolve the sulfide minerals with saturated bromine water, which results in the remaining insoluble substance becoming insoluble (such as jarosite).The leach residue was analyzed by this method, and the contents of iron sulfide and sulfate in the residue sample such as in jarosite was determined [21,22].

3. Results and Discussion

3.1. Effect of Temperature on Zinc and Iron Extraction

Test conditions were as follows: oxygen partial pressure was maintained at 0.5 MPa, leaching time 2 h, L/S 5:1, H_2SO_4/Zn ratio 1.1:1, initial acid concentration 183.9 g/L, lignin addition amount 0.2 g, stirring speed 500 rpm, −325 mesh which accounts for 93% of the milled concentrate. The effect of temperature on the extraction of Fe and Zn during the pressure leaching of zinc sulfide concentrate was examined. The test results are shown in Figure 3.

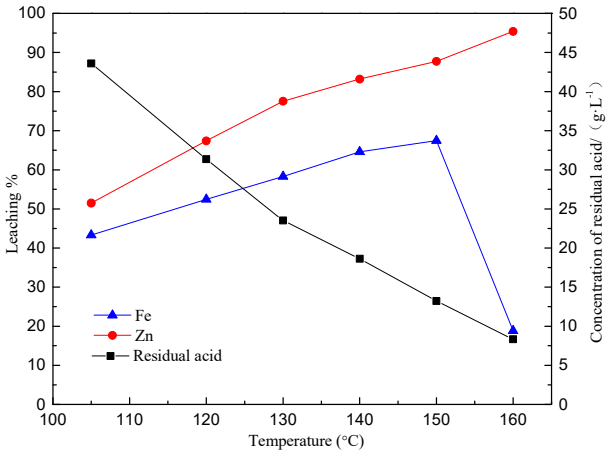

Figure 3. Effect of the leaching temperature on the extractions of Zn and Fe.

It can be seen from Figure 3 that the zinc extraction is proportional to the temperature. The iron extraction first increases with increase in the temperature and then decreases when the temperature exceeds 150 °C. The dominant behavior of iron then becomes hydrolysis to form precipitates, consequently leading to the lower net iron extraction.

Figure 4 exhibits the XRD patterns of the leach residues formed at different temperatures. As seen in the figure, the residue mainly contains zinc sulfide and elemental sulfur at the temperature of 120 °C. As the temperature rises, the intensity of the zinc sulfide phase gradually decreases. When the temperature reaches 160 °C, the lead jarosite phase appears, the intensity of the elemental sulfur phase decreases slightly, and the intensity of zinc sulfide phase drops significantly. These observations are all consistent with the increasing zinc extraction as a function of temperature.

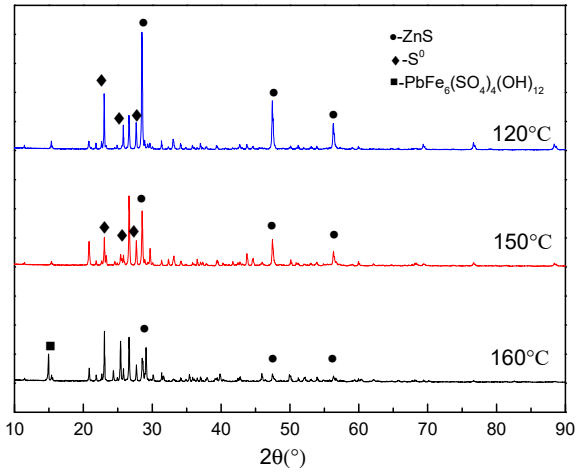

Figure 4. XRD patterns of residue under different temperature conditions.

The leach residue under varying temperature conditions was analyzed using chemical phase analysis. When the temperature is within the range of 105 to 150 °C, the contents of insoluble iron phases are low and remains basically constant, as shown in Figure 5. When the temperature exceeds 150 °C, the content of insoluble iron phases spikes considerably, which is consistent with the formation of Pb-jarosite in large amounts resulting from the hydrolysis of iron in the solution above 150 °C.

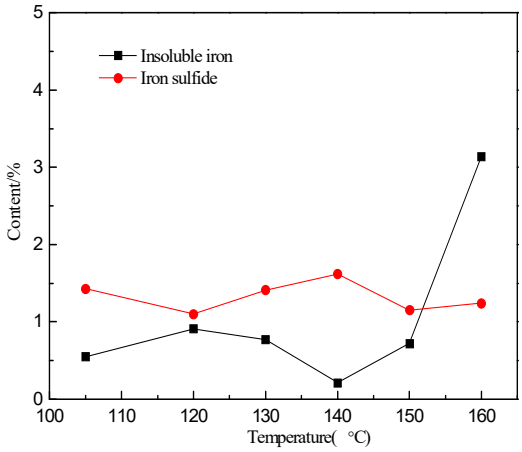

Figure 5. The content of different iron phase in the leach residue at different temperatures.

It is clearly observed in Figure 6 that the decomposition of iron-containing minerals always increases with temperature. When the temperature reaches 105 °C, the decomposition of iron-containing minerals is 61%. When the temperature reaches 160 °C, the decomposition of iron-containing minerals increases up to 78%. Concurrently, the iron precipitation increases substantially when the leaching temperature attains 160 °C. It is stable and remains just above or below 15% in the temperature range of 105 to 150 °C, then increases afterwards to 56% when the temperature augments to 160 °C. When the temperature is lower than 150 °C, the iron in the zinc sulfide concentrate is significantly dissolved. When the temperature is above 150 °C, the dissolved iron is increasingly controlled by the hydrolysis and precipitation reactions, forming a significant amount of iron precipitates. Therefore, increasing the temperature to 150 °C does not only promote the leaching of sulfide ores, but also facilitates the hydrolysis and precipitation of iron, which is conducive to the separation of dissolved zinc from iron.

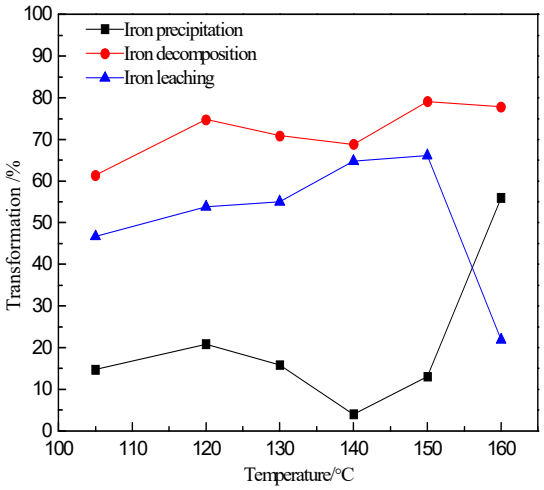

Figure 6. Relation between the iron extraction and extent of iron precipitation with temperature.

3.2. Effect of Acidity on Zinc and Iron Extractions

The test conditions were set as follows: temperature 150 °C, oxygen partial pressure 0.5 MPa, leaching time 2 h, L/S 5:1, mass of added lignin 0.2 g, stirring speed 500 rpm, particles size of −325 mesh, which accounts for 93%. The influence of acidity on the extractions of Fe and Zn during the pressure leaching process of zinc sulfide concentrates was investigated. The test results are presented in Figure 7.

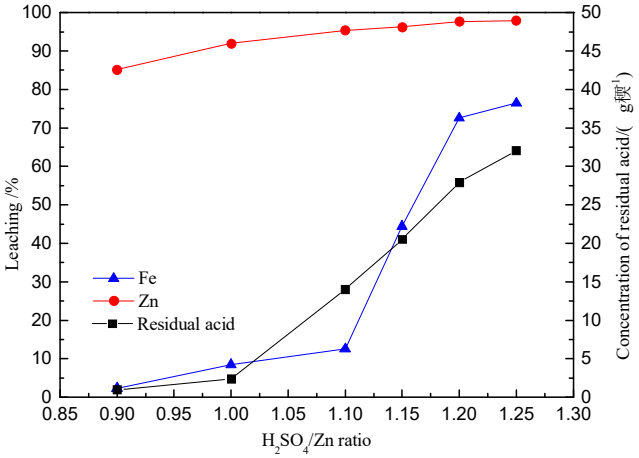

Figure 7. Effect of H_2SO_4/Zn on the extractions of Zn and Fe.

Figure 7 confirms that both the zinc and iron extraction increase with a corresponding increase in the H_2SO_4/Zn ratio. When the H_2SO_4/Zn ratio increases to 1.2:1, the zinc extraction slowly increases and tapers to a value of 98%. Therefore, it can be concluded that zinc can be effectively leached when the H_2SO_4/Zn ratio is 1.2:1. Additionally, as the H_2SO_4/Zn ratio increases, a sharp increase in the iron extraction is observed. Further increasing the H_2SO_4/Zn ratio to 1.25 demonstrates a slight increment in the iron extraction.

Figure 8 exhibits the XRD patterns of the residue obtained with different acidities. As shown in Figure 8, the leach residue mainly contains ZnS, S^0 and Pb-jarosite when the H_2SO_4/Zn ratio is 1.1. When the H_2SO_4/Zn ratio increases to 1.2, ZnS and S^0 phases become dominant in the leach residue with the absence of Pb-jarosite. These results confirm that the formation of jarosite through hydrolysis of ferric ions is inhibited due to the increased acidity, which is consistent with the subsequent increase of the iron extraction.

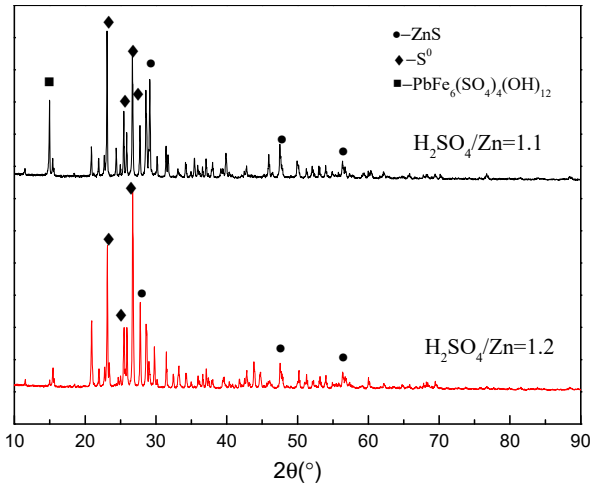

Figure 8. XRD patterns of residues with different acidities.

Figure 9 shows the results for chemical phase analysis of the leach residue. It can be depicted from the above figure that the iron content in the sulfide minerals decreases as the solution becomes more acidic. However, the change above a ratio of 1.1:1 does not contribute significantly to the extra iron extraction. The contents of the insoluble iron first increases gradually in the H_2SO_4/Zn ratio range of 0.9~1, and then progressively decreases within H_2SO_4/Zn ratios of 1~1.25. This can be explained by the fact that the low acidity within the ratios of H_2SO_4/Zn 0.9~1 is beneficial to hydrolysis, which promotes the formation of Pb-jarosite and leads to an increase of insoluble iron (lead jarosite). The high acidity ranges, i.e., the ratio of H_2SO_4/Zn in the range of 1~1.25, is not conducive to the formation of lead jarosite.

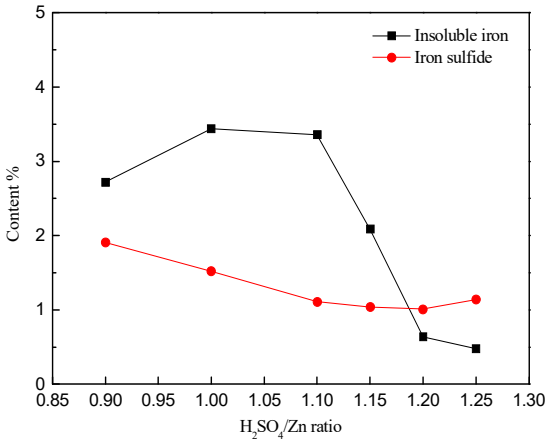

Figure 9. The content of different iron phase in the leaching residue with different H_2SO_4/Zn ratios.

It can be observed from Figure 10 that the decomposition of iron containing minerals increases with increase in the H_2SO_4/Zn ratio. Decomposition increases from 61% to 84% for the H_2SO_4/Zn ratio, increasing from 0.9:1 to 1.2:1. The iron precipitation increases initially and then decreases with an increase in the H_2SO_4/Zn ratio. When the ratio of H_2SO_4/Zn is within (0.9~1):1, the iron precipitation increases from 56% to 65%. When the H_2SO_4/Zn ratio further increases to 1.25:1, the iron precipitation plummets to 7.6%. Figure 10 suggests that increasing the H_2SO_4/Zn ratio promotes the decomposition of, and extraction from, iron containing minerals. However, the precipitation of ferric ions increases only at a low acid level. As the ratio of H_2SO_4/Zn approaches 1:1, the precipitation decreases. In the range of H_2SO_4/Zn ratio (0.9~1):1, the decomposition and leaching processes of the iron containing minerals are similar. When the H_2SO_4/Zn ratio is in the range of (1.1~1.25):1, the decomposition and leaching processes of iron containing minerals become more dominant.

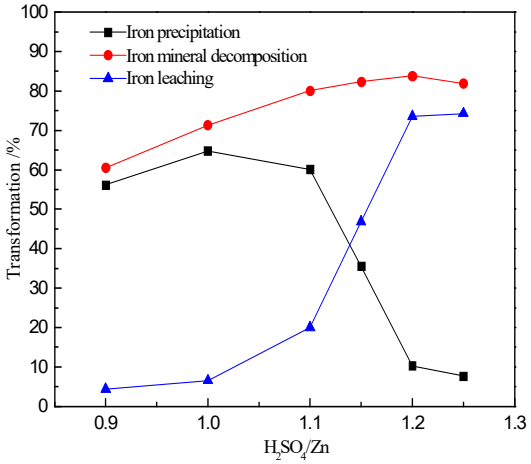

Figure 10. Relationship between extraction, iron decomposition and iron precipitation at various H_2SO_4/Zn ratios.

3.3. Effect of Leaching Time on Zinc and Iron Extractions

Test conditions were configured as follows: temperature 150 °C, oxygen partial pressure 0.5 MPa, H_2SO_4/Zn: 1.1:1, L/S 5:1, initial acid concentration 183.9 g/L, mass of added lignin 0.2 g, stirring speed 500 rpm, −325 mesh accounts for 93%. The effects of leaching time on the extractions of Fe and Zn during the pressure leaching of the zinc sulfide concentrates were investigated. The leaching times were 0.5, 1, 1.5, and 2 h, respectively. The results are illustrated in Figure 11.

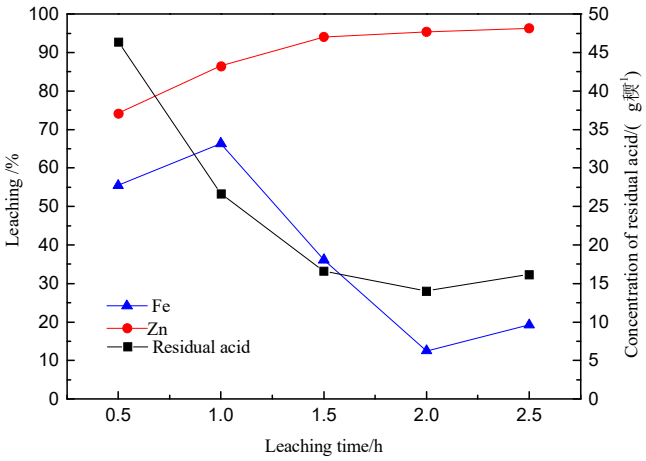

Figure 11. Effect of leaching time on extractions of Zn and Fe.

It can be seen from Figure 11 that the zinc extraction was proportional to the leaching duration. After a prolonged duration of 1.5 h, the zinc extraction reached 94% and then plateaued. On the other hand, the iron extraction increased at first and then decreased with respect to the leaching duration. When the time extends to 1 h, the highest extraction for iron of 66% was reached. Prolonging the time to 2.5 h, the iron extraction gradually decreases. This confirms that the dissolution of iron containing minerals tend to dominate when the leaching time is less than 1 h. As the leaching time increases, the dissolved ferrous ions are oxidized and subsequently hydrolyzed to form precipitates, hence the accompanying decline of the iron extraction.

Figure 12 reveals that the leach residue mainly contains ZnS, S^0 and Pb-jarosite when the leaching time is 0.5 h. As the leaching time is prolonged, the intensity of the ZnS phase gradually decreases while the intensity of the S phase progressively increases. When the duration is extended to 2 h, the Pb-jarosite phase appears and the intensity of the ZnS phase decreases significantly.

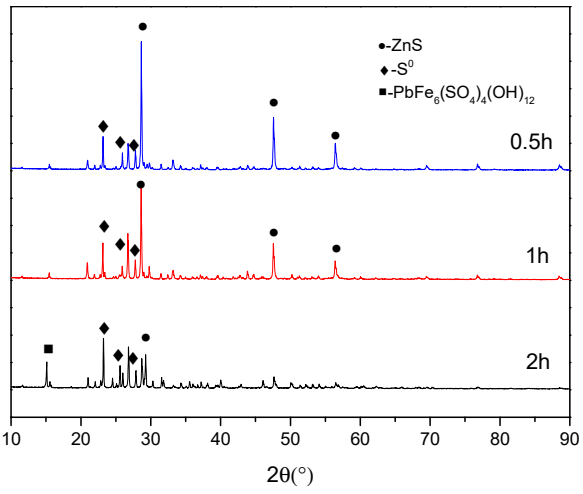

Figure 12. XRD patterns of leach residues with different leaching times.

As shown in Figure 13, the iron content in the sulfide minerals steadily declines with the leaching time. The content of insoluble iron increases considerably starting from 1 h, indicating that hydrolysis begins after 1 h and forms lead jarosite.

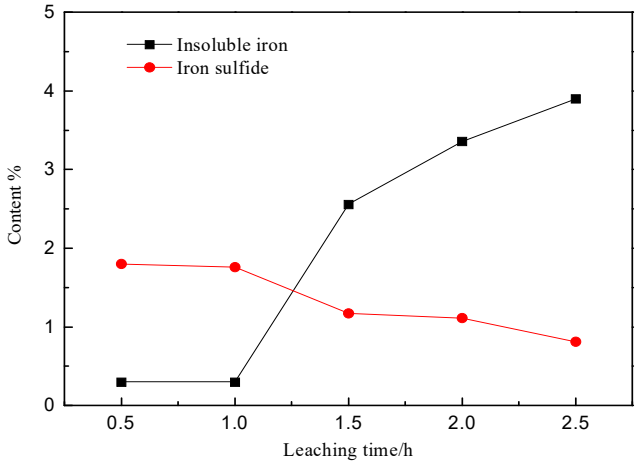

Figure 13. The content of different iron phase in the leach residue with the leaching time.

The decomposition of iron minerals increases with the leaching time, as shown in the Figure 14. When the leaching time is 0.5 h, the iron minerals decomposition reaches 61%. Extending the time to 2.5 h, the decomposition of iron minerals further increases to 86%. The iron precipitation increases significantly over a certain time period. When the leaching time is less than 1 h, the iron precipitation is about 6%. When the time is extended to 2.5 h, the iron precipitation reaches a maximum of 69%. It can be deduced that prolonging the leaching time increases the decomposition of iron minerals and the precipitation of ferric iron, which in turn can decrease the net iron extraction. The minerals are mainly decomposed and leached within 1 h of the reaction. The ferric iron begins to precipitate after the reaction time exceeds 1 h.

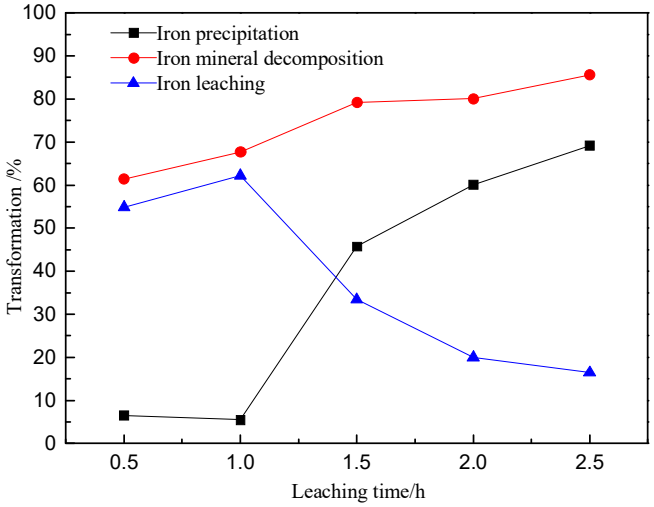

Figure 14. Relation between the extraction and extent of precipitation of iron as a function of the leaching time.

3.4. Phase Analysis of Residues

3.4.1. Morphology Analysis

The leach residue obtained at leaching temperatures of 150 and 160 °C and leaching durations of 0.5 and 2.5 h were selected and explored by SEM. The results are revealed below: Figure 15 SEM images

of the leach residues obtained at leaching temperatures of 150 and 160 °C, respectively. Spherical particles are observed in the 150 °C sample, whilst irregular blocks and needle-like substances adhering to the surface are exhibited in the 160 °C sample.

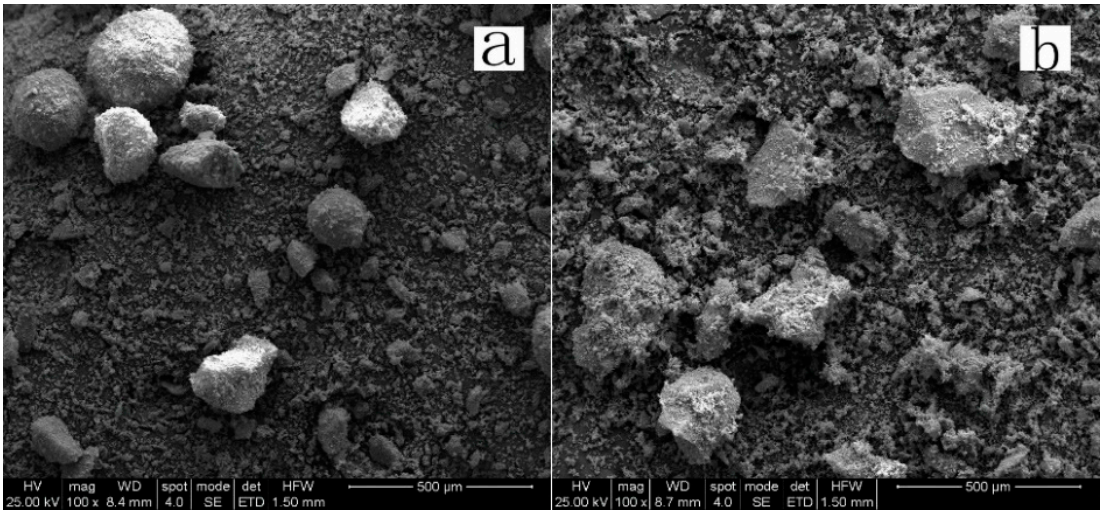

Figure 15. SEM images of residues (**a**) leaching temperature of 150 °C; (**b**) leaching temperature of 160 °C.

Figure 16 is a set of SEM pictures of the leach residue with leaching times of 0.5 and 2.5 h, respectively. It shows that when the leaching time is 0.5 h, there is no obvious agglomeration and few particles are observed on the surface. When the leaching time increases to 2.5 h, the agglomeration becomes more evident with more fine particles distributed on the surface.

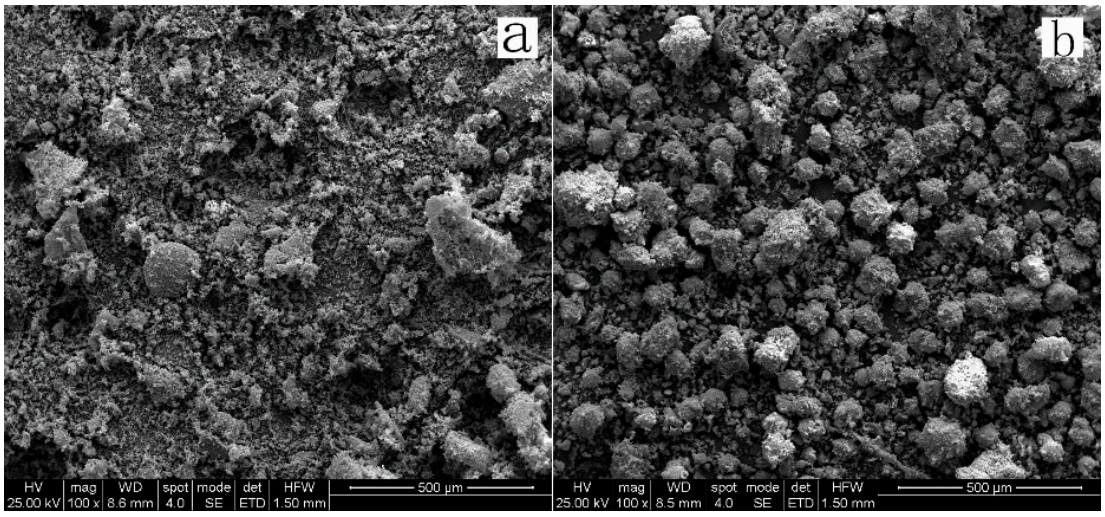

Figure 16. SEM images of residues (**a**) leaching time 0.5 h; (**b**) leaching time 2.5 h.

3.4.2. EDS Analysis

Scanning electron microscopy and EDS analysis were performed on the leach residue. The information in Figures 17 and 18 illustrates the analysis results for leach residues obtained at a temperature of 150 °C. Figures 17 and 18 show that the spherical particles are mostly composed of elemental sulfur. The residual sphalerite and pyrite are present both inside and at the surface of the sulfur particles. No Pb-jarosite phase is identified in the SEM images after EDS analysis. Rather, the presence of residual galena surrounded by a coating of lead sulphate was found (Figure 18).

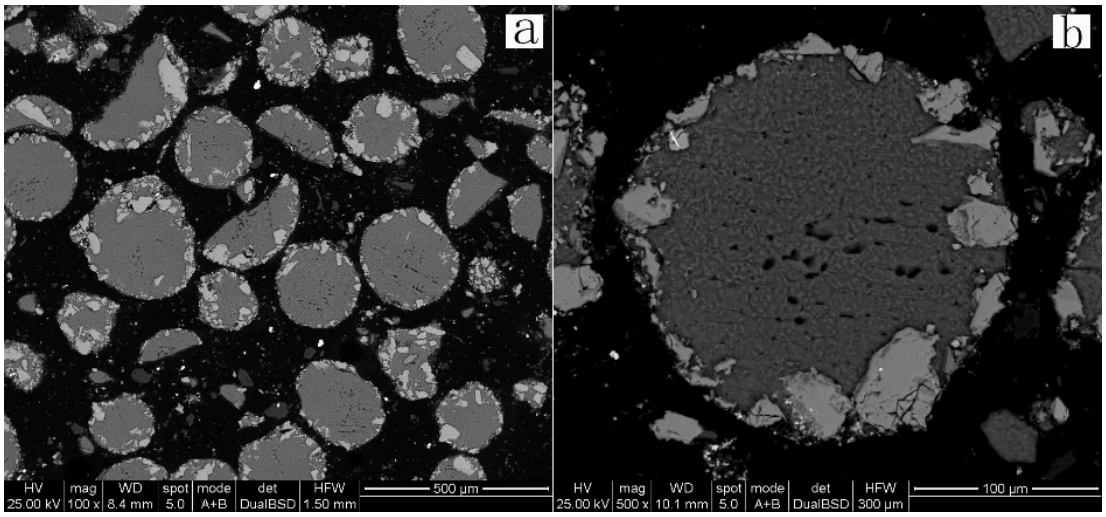

Figure 17. BSE images of 150 °C leach residues. Scale: (**a**) 500 µm; (**b**) 100 µm.

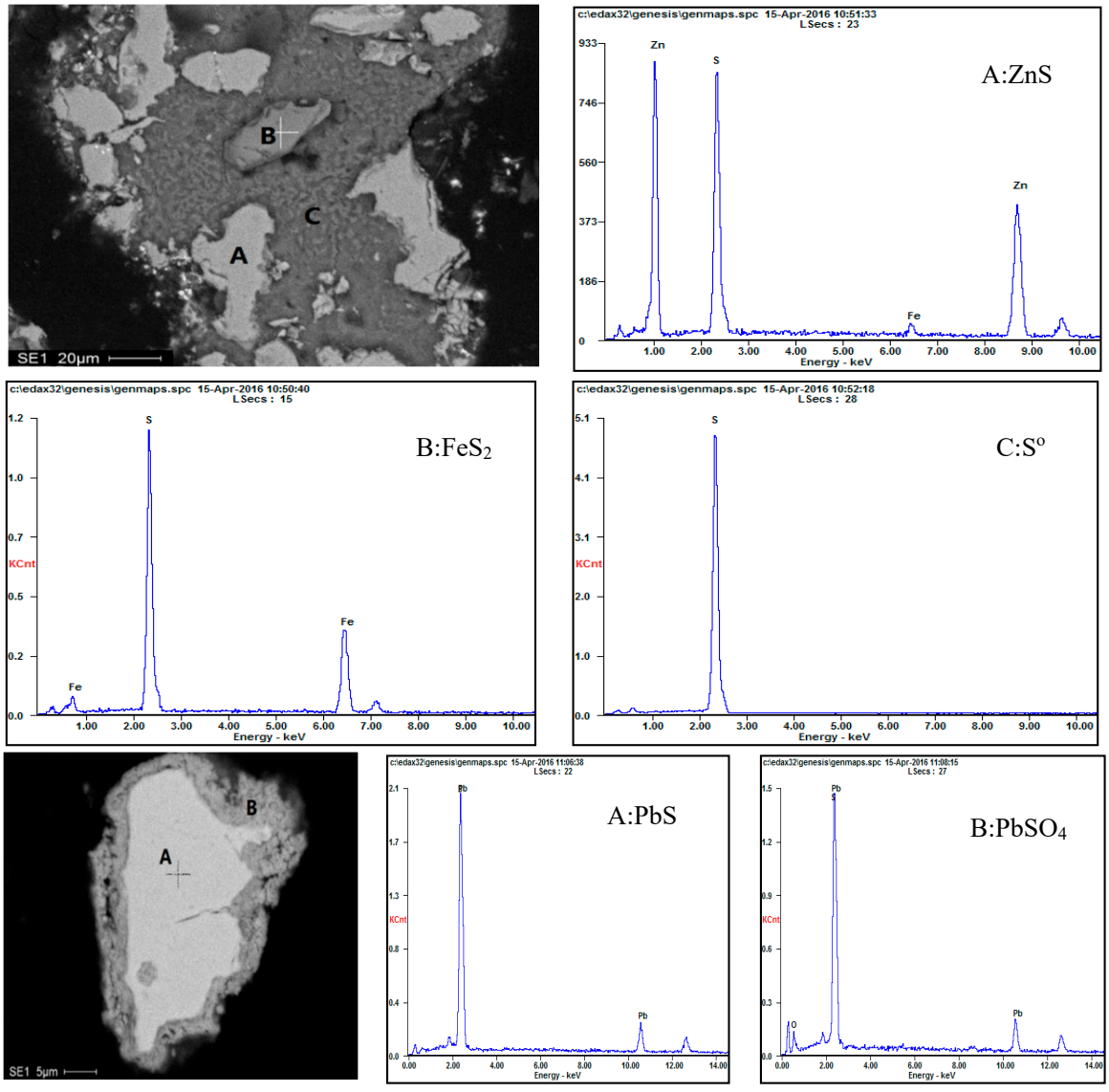

Figure 18. SEM and EDS spectra for the leach residue obtained at 150 °C.

Figure 19 demonstrates the results for leach residues obtained at a temperature of 160 °C. It shows that the irregular shaped particles are primarily elemental sulfur. Small amounts of residual minerals are embedded inside and at the edge of the elemental sulfur particles (Figure 19a). Fine particles surround the elemental sulfur particles (Figure 19b), which are identified as Pb-jarosite by EDS analysis (Figure 20). Figure 19c shows that the quartz is joined to the Pb-jarosite formed at 160 °C.

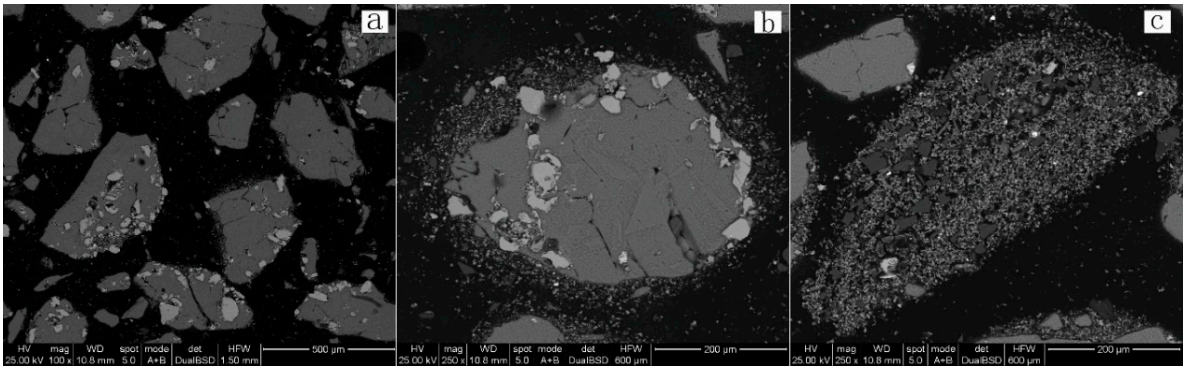

Figure 19. BSE images of 160 °C leach residue. Scale: (**a**) 500 µm; (**b**) 200 µm; (**c**) 200 µm.

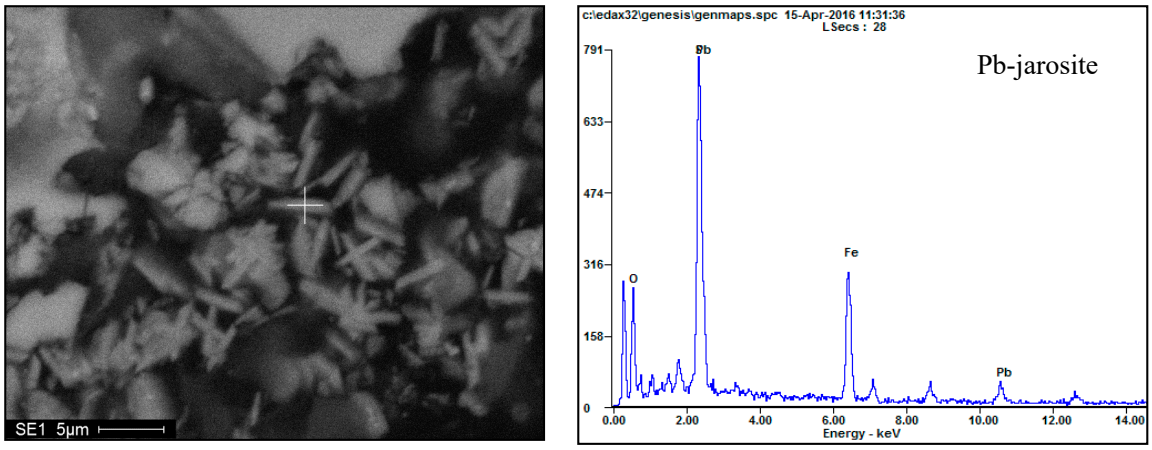

Figure 20. SEM and EDS spectrum for the leach residue obtained at 160 °C.

It is expected that the ferric ions leached from iron minerals at 160 °C are mainly hydrolyzed to form Pb-jarosite, which can occur in two ways. First, the ferric cations in the solution form Pb-jarosite near the exterior of the mineral edge. Second, the free ferric ions formed by gradual dissolution are in contact with $PbSO_4$, which are then hydrolyzed to form Pb-jarosite, replacing $PbSO_4$ and becoming joined to quartz.

Figure 21 is a SEM image of the residue samples for leaching times of 0.5 and 2.5 h, respectively. It is observed that the elemental sulfur is of spherical or irregular shape, with residual minerals attached to its periphery. Comparing the four images, the sulfur particles formed after a leaching time of 2.5 h are significantly larger than after a leaching duration of 0.5 h. Furthermore, the elemental sulfur content increased, and the residual minerals content was reduced.

EDS spectra of residue samples after leaching times of 0.5 and 2.5 h are exhibited in Figure 22a,b, respectively. Figure 22a shows the lead sulfate produced from the dissolution of galena after 0.5 h. Figure 22b exhibits an intimate body of Pb-jarosite and quartz. No lead sulfate was identified in the 2.5 h sample. This is consistent with the conversion of lead sulfate to lead jarosite as the reaction proceeds.

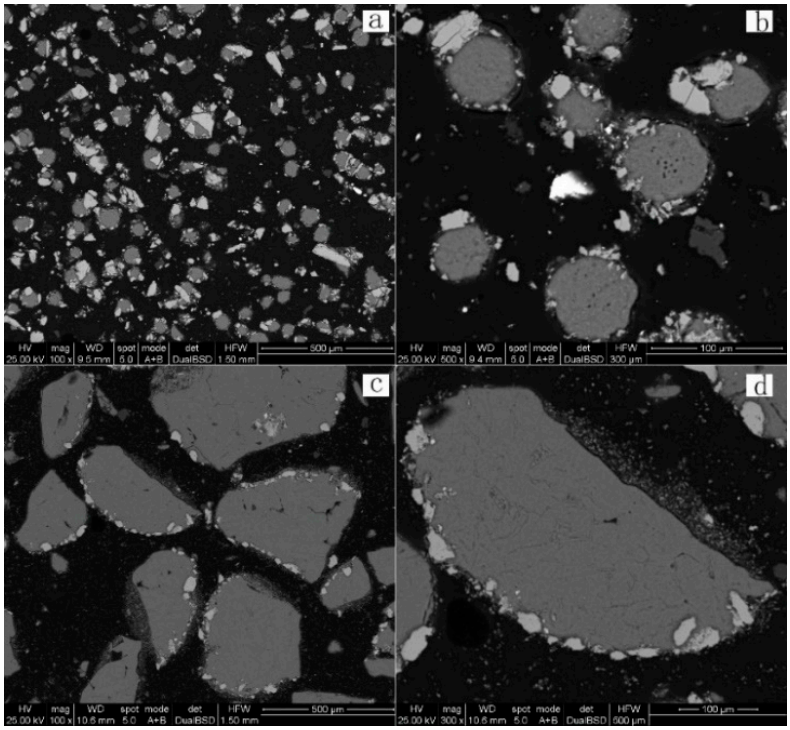

Figure 21. BSE images of leach residues (**a**,**b**) leaching time of 0.5 h; (**c**,**d**) leaching time of 2.5 h.

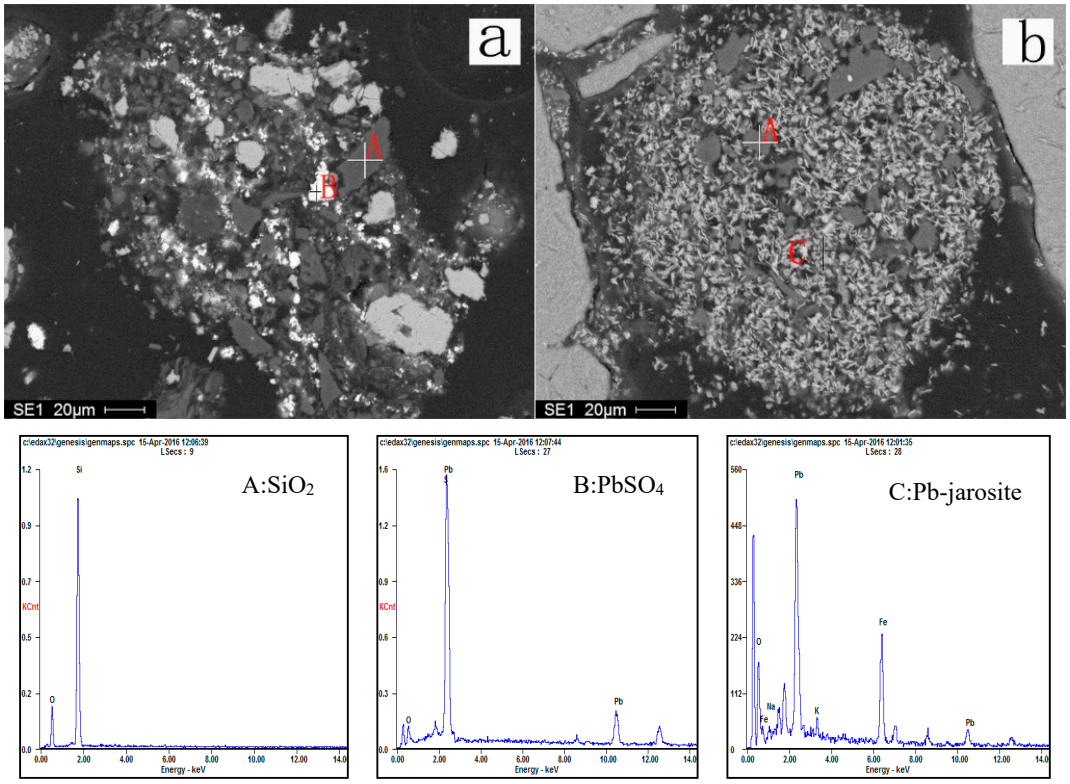

Figure 22. SEM images and EDS spectrum of leach residues (**a**): leaching time 0.5 h; (**b**): leaching time 2.5 h.

4. Conclusions

In this paper, the behavior of iron during the leaching of zinc sulfide concentrates was studied in detail. The research demonstrated that temperature, acidity, and leaching time all have an influence on the extractions of zinc and iron. Under the experimental conditions investigated, the extraction of zinc increased with temperature, acidity, and leaching time. The zinc extraction reached 97% under set conditions of temperature 150 °C, H_2SO_4/Zn ratio 1.2:1, and leaching time 2 h. The iron extraction was also demonstrated to vary with temperature, acidity and leaching time. Its specific behavior can be described as follows:

The iron extraction increased with temperature up to 150 °C, and then decreased when the temperature rose further to 160 °C.

1. The iron extraction increased with the ratio of H_2SO_4/Zn within the range of 0.9:1 to 1.25:1; however, most rapidly in the range 1.0:1 to 1.2:1.
2. The iron extraction displayed an initial increase that was followed by a decrease, with respect to the leaching time.

The leach residues were analyzed using a chemical phase analysis method. The relationship between the extent of decomposition and extraction of iron minerals, and the extent of iron precipitation was quantitatively studied in detail. Under the conditions investigated in this study, the extent of decomposition of iron minerals was shown to increase with temperature, H_2SO_4/Zn ratio, and leaching time. The extent of decomposition was within the range 60.4%~85.6%. In contrast, the variation of iron precipitation is more complicated as the conditions change. The results were as follows:

1. The precipitation of iron increased sharply from approximately 15.0% to 55.9% when the temperature exceeds 150 °C.
2. The precipitation of iron increased initially to a maximum of 64.8% (H_2SO_4/Zn = 1:1) and then decreased to its lowest value of 7.63% (H_2SO_4/Zn = 1.25:1).
3. The precipitation of iron was maintained at about 6% (for leaching time ≤ 1 h). Subsequently, it increased quite markedly and reached the highest value of 69.2% (after leaching time = 2.5h).

Evidence from the EDS analysis indicates that there are two mechanisms for lead jarosite to form. First, ferric ions in the solution form Pb-jarosite near the exterior of the iron- containing galena mineral edge. Second, the free ferric ions come into contact with $PbSO_4$ to form Pb-jarosite, which replaces the $PbSO_4$ to form an intimate mixture with quartz.

In summary, the results show that increasing the leaching temperature, appropriately reducing the H_2SO_4/Zn ratio, and prolonging the leaching time are all beneficial to the separation of Zn and Fe. The iron minerals in the zinc sulfide concentrate are mainly oxidized and leached at the lower temperature and in the early stages of the reaction. The precipitation of iron occurs subsequent to leaching. When the reaction employs specific experimental conditions (temperature of 150 °C, leaching time of 2.5 h), the hydrolytic precipitation of iron dominates. Under weaker acidic conditions, i.e., the H_2SO_4/Zn ratio is (0.9~1):1, the decomposition and leaching of iron minerals are similar to the precipitation of ferric ions. Under conditions of high acidity with H_2SO_4/Zn ratio of (1~1.25:1), iron containing mineral decomposition and leaching dominates and the iron reports to leaching residues in the form of Pb-jarosite.

Author Contributions: K.-X.J. and H.-B.W. have been leading the research project, obtaining funding acquisition and conceptualization as well as writing—review and editing. S.-C.Q. has designed, conducted the experiments and put this work on paper. B.-S.Z., Y.-F.W. and X.-D.Z. have been writing-review and editing. All authors have read and agreed to the published version of the manuscript.

Funding: This work was financially supported by the National Natural Science Foundation of China (No.51434001 and No.51574034), and National Key Research and Development Plan of China (2018YFC1900401).

Conflicts of Interest: The authors declare no conflict of interest.

References

1. Liao, M.; Deng, T. Zinc and lead extraction from complex raw sulfides by sequential bioleaching and acidic brine leach. *Miner. Eng.* **2004**, *17*, 17–22. [CrossRef]
2. Santos, S.M.C.; Machado, R.M.; Correia, M.J.N.; Reis, M.T.A.; Ismael, M.R.C.; Carvalho, J.M.R. Ferric sulphate/chloride leaching of zinc and minor elements from a sphalerite concentrate. *Miner. Eng.* **2010**, *23*, 606–615. [CrossRef]
3. Souza, A.D.; Pina, P.S.; Leao, V.A. Bioleaching and chemical leaching as an integrated process in the zinc industry. *Miner. Eng.* **2007**, *20*, 591–599. [CrossRef]
4. Souza, A.D.; Pina, P.S.; Leao, V.A.; Silva, C.A.; Siqueira, P.F. The leaching kinetics of a zinc sulphide concentrate in acid ferric sulphate. *Hydrometallurgy* **2007**, *89*, 72–81. [CrossRef]
5. Sahu, S.; Sahu, K.; Pandey, B. Leaching of zinc sulfide concentrate from the ganesh-himal deposit of Nepal. Metall. Mater. Trans. B: Process Metall. *Mater. Process. Sci.* **2006**, *37*, 541–549.
6. Owusu, G.; Dreisinger, D.B.; Peters, E. Effect of surfactants on zinc and iron dissolution rates during oxidative leaching of sphalerite. *Hydrometallurgy* **1995**, *38*, 315–324. [CrossRef]
7. Han, J.; Liu, W.; Qin, W.; Peng, B.; Yang, K.; Zheng, Y. Recovery of zinc and iron from high iron-bearing zinc calcine by selective reduction roasting. *Ind. Eng. Chem.* **2015**, *22*, 272–279. [CrossRef]
8. Nikkhou, F.; Xia, F.; Deditius, A.P. Variable surface passivation during direct leaching of sphalerite by ferric sulfate, ferric chloride, and ferric nitrate in a citrate medium. *Hydrometallurgy* **2019**, *188*, 201–215. [CrossRef]
9. Ghassa, S.; Noaparast, M.; Shafaei, S.Z.; Abdollahi, H.; Gharabaghi, M.; Boruomand, Z. A study on the zinc sulfide dissolution kinetics with biological and chemical ferric reagents. *Hydrometallurgy* **2017**, *171*, 362–373. [CrossRef]
10. Koerker, F.W.; Calderwood, H.N. The system ferric oxide-sulfur trioxide-water. *J. Phys. Chem.* **2002**, *42*, 1151–1155. [CrossRef]
11. Hasegawa, F.; Tozawa, K.; Nishimura, T. Solubility of ferrous sulfate in aqueous solutions at high temperatures. *J. Min. Mater. Process. Inst. Jpn.* **1996**, *112*, 879–884.
12. Umetsu, V.; Tozawa, K.; Sasaki, K. The hydrolysis of ferric sulphate solutions at elevated temperatures. *Can. Metall. Quart.* **1977**, *16*, 111–117. [CrossRef]
13. Chen, Z.; He, X. Zinc concentrate oxygen pressure leaching technology. *Hum. Nonferrous Met.* **2002**, *18*, 26–28.
14. Tang, J.; Zhou, X. Behavior of iron in the process of pressure leaching of zinc sulfide concentrate. *Non Ferr. Met. (Smelt. Part)* **1987**, *3*, 32–35.
15. Posnjak, E.; Merwin, H.E. The system Fe_2O_3-SO_3-H_2O. *J. Am. Chem. Soc.* **1922**, *44*, 1965–1994. [CrossRef]
16. Yue, M.; Sun, N.; Zou, X.; Shao, J.; Liu, J.; Wang, K.; Lu, Y. The discussion on hydrolysis precipitation of ferric oxide directly from ferric-ion rich zinc leachate. *China Nonferrous Metall.* **2012**, *4*, 80–85.
17. Ruiz, M.C.; Zapata, J.; Padilla, R. Effect of variables on the quality of hematite precipitated from sulfate solutions. *Hydrometallurgy* **2007**, *89*, 32–39. [CrossRef]
18. Dutrizac, J.E. Converting jarosite residues into compact hematite products. *JOM* **1990**, *42*, 36–39. [CrossRef]
19. Ghassa, S.; Noaparast, M.; Shafaei, S.Z.; Abdollahi, H.; Gharabaghi, M.; Boruomand, Z. Medium-pressure test of zinc sulfide pressure leaching. *Sulfuric Acid Ind.* **1983**, *4*, 50–55.
20. Xu, Z.; Jiang, Q.; Wang, C. Behavior of zinc, sulfur and iron during low temperature pressure leaching of iron sphalerite. *Non Ferr. Met. (Smelt. Part)* **2012**, *7*, 6–11.
21. Beijing Research Institute of Mining and Metallurgy. *Chemical Phase Analysis*; Metallurgical Industry Press: Beijing, China, 1976.
22. Qin, S.; Jiang, K.; Zhang, B.; Wang, H. Study on phase form and content of Sulfur and Iron in leaching residue of oxygen pressure leaching of sphalerites. *Chin. J. Inorg. Anal. Chem.* **2016**, *6*, 57–61.